

**Original Research**

**Can we predict the neutral breast position using the gravity-loaded breast position, age, anthropometrics and breast composition data?**

<sup>1,2</sup>Michelle Norris<sup>ORCID iD</sup>\*, <sup>2,3</sup>Aoife O'Neill<sup>ORCID iD</sup>, <sup>4</sup>Tim Blackmore<sup>ORCID iD</sup>, <sup>4</sup>Chris Mills<sup>ORCID iD</sup>, <sup>4</sup>Amy Sanchez<sup>ORCID iD</sup>,  
<sup>5</sup>Nicola Brown<sup>ORCID iD</sup> and <sup>4</sup>Joanna Wakefield-Scurr<sup>ORCID iD</sup>.

<sup>1</sup>Lero, the Science Foundation Ireland Research Centre for Software, University of Limerick, Limerick, Ireland.

<sup>2</sup>Ageing Research Centre (ARC), Health Research Institute (HRI), University of Limerick, Limerick, Ireland.

<sup>3</sup>School of Allied Health, University of Limerick, Limerick, Ireland.

<sup>4</sup>School of Sport, Health and Exercise Science, Spinnaker Building, University of Portsmouth, United Kingdom.

<sup>5</sup>Faculty of Sport, Health and Applied Science, St. Mary's University, Waldegrave Road, Twickenham, United Kingdom.

\*Address for correspondence:

Michelle Norris

Lero, the Science Foundation Ireland Research Centre for Software,

Tierney Building,

University of Limerick,

Ireland.

Email: michelle.norris@lero.ie

**Abstract Word Count: 246**

**Main Text Word Count: 4,491**

## Abstract

*Background:* This study aimed to identify the predictor variables which account for neutral breast position variance using a full independent variable dataset (the gravity-loaded breast position, age and anthropometrics, and magnetic resonance imaging breast composition data), and a simplified independent variable dataset (magnetic resonance imaging breast composition data excluded).

*Methods:* Breast position (three-dimensional neutral and static gravity-loaded), age, anthropometrics and magnetic resonance imaging breast composition data were collected for 80 females (bra size 32A to 38D). Correlations between the neutral breast position and the gravity-loaded breast position, age, anthropometrics, and magnetic resonance imaging breast composition data were assessed. Multiple linear and multivariate multiple regression models were utilised to predict neutral breast positions, with mean absolute differences and root mean square error comparing observed and predicted neutral breast positions.

*Findings:* Breast volume was the only breast composition variable to contribute as a predictor of the neutral breast position. While  $\geq 69\%$  of the variance in the anteroposterior and mediolateral neutral breast positions were accounted for utilising the gravity-loaded breast position, multivariate multiple regression modelling resulted in mean absolute differences  $>5$  mm.

*Interpretation:* Due to the marginal contribution of breast composition data, a full independent variable dataset may be unnecessary for this application. Additionally, the gravity-loaded breast position, age, anthropometrics, and breast composition data do not successfully predict the neutral breast position. Incorporation of the neutral breast position into breast support garments may enhance bra development. However, further identification of variables which predict the neutral breast position is required.

**Keywords:** Breast composition, skin strain, breast position, garment development.

## 1. Introduction

During dynamic movement, independent breast motion and the associated breast pain can be reduced with the application of external breast support (Zhou et al., 2011). Recently, research has proposed that breast support garment development could be improved by controlling the effects of gravity on the breast (Mills et al., 2016). Sanchez et al., (2017) defined the neutral breast position as the position in which breast skin is not under gravitational loading (unloaded), with the breast therefore optimally positioned in terms of minimising the risk of exceeding breast skin strain limits (Sanchez et al., 2017). Any breast support garment which initially positions the breast in the neutral breast position, may act protectively in limiting breast skin strain values within their reversible deformation limits (Silver et al., 2001).

Previous research has estimated the neutral breast position using 3D motion capture of the breast during water and soybean oil immersion (Mills et al., 2016; Sanchez et al., 2017), or water immersion alone (Norris et al., 2020, 2018). However, to the author's knowledge no attempt has been made to predict the neutral breast position. Predictive regression analysis in breast biomechanics has primarily focused on the prediction of breast volume (Koch et al., 2011), breast deformations after breast conserving surgery (Zolfagharnasab et al., 2018), upper torso musculoskeletal pain (Coltman et al., 2018) and breast mass (Brown et al., 2012). Regardless, when conducting regression analysis, consideration must be given to (1) the identification of relevant independent (predictor) variables which ensure model accuracy and (2) the elimination of unnecessary independent (predictor) variables which allows for simplified future data collection without compromising model accuracy (Halinski and Feldt, 1970), and in this case may improve the ability to utilise the prediction model within the bra industry.

Firstly, to appropriately identify relevant independent predictor variables there must be an understanding of the factors which influence the neutral breast position. As the neutral breast position estimates the non-gravity-loaded breast position (Mills et al., 2016), it is likely that gravity-loaded breast position is of importance in this prediction model. Additionally, characteristics which help to inform the static, two-dimensional (2D) gravity-loaded breast position, such as breast ptosis and splay, may also influence the neutral breast position. To date it has been stated that breast composition

variables such as breast mass (of more than 400 grams), ligamentous laxity, previous weight loss, postoperative changes, dermatochalasis, and glandular hormonal regression (postpartum or menopausal) are all causes of breast ptosis (Georgiade et al., 1990; Regnault, 1976; Rinker et al., 2010). Those displaying greater breast splay generally display hypertrophic breast volumes and increased ptosis, whilst breast splay is also thought to be related to participants age and body mass index (BMI) (Coltman et al., 2018). Furthermore, measures of body fat, such as the sum of eight skinfolds, have been identified to display a positive relationship with breast mass (Brown et al., 2012). It may therefore be important to consider age and anthropometrics, when predicting the neutral breast position. Previously, magnetic resonance imaging (MRI) has been utilised to assess breast volume and composition, including breast tissue differentiation (Graham et al., 1996; Klifa et al., 2010), breast volume assessment (Herold et al., 2010) and breast density estimation (Nie et al., 2008). MRI is therefore a recognised method of estimating breast volume and composition, both of which may be related to the neutral breast position.

It is also important to ensure that unnecessary independent (predictor) variables are excluded from regression models, to improve the ability to implement the prediction model within the bra industry. Gravity-loaded breast characteristics and participant anthropometrics are already utilised within the bra industry, with both Victoria's Secret® and Rigby and Peller® utilising 3D body scanning to identify breast characteristics (bust shape) (McCann and Bryson 2014) and participant anthropometrics (140 upper body measurements) (Rigby and Pellar, 2022) to inform bra size. These variables may therefore not add increased complication within bra development processes. While MRI breast composition data may be costly to obtain (Caruso et al., 2006), it is not yet known if it enhances neutral breast position prediction. Establishing this would help identify if current variables utilised within the bra development process, are sufficient when predicting the neutral breast position, or if MRI breast composition is required.

Therefore, this novel study firstly aimed to utilise regression modelling to identify the predictor variables which account for neutral breast position variance using a full independent variable dataset

(the gravity-loaded breast position, age and anthropometrics, and MRI breast composition data), and a simplified independent variable dataset (MRI breast composition data excluded). This study then aimed to assess model prediction accuracy, with a threshold of 5 mm (Hansson et al., 2014).

## **2. Methods**

Data collection consisted of two testing sessions; (1) a laboratory testing session which included a professional bra fit, anthropometric assessment and static breast measurements and (2) a hospital-based breast MRI. Participants were required to complete the laboratory testing session and breast MRI (in any order) within 48 hours of each other to minimise any breast changes (Fowler et al., 1990).

### **2.1 Participants**

Following institutional ethical approval (SFEC 2018-109, Science Faculty Ethics Committee, University of Portsmouth, Portsmouth, United Kingdom), 80 females gave written informed consent to participate. Participants were (median and range) aged 25 years (18 to 37 years) with a BMI of 24.1 kg/m<sup>2</sup> (16.9 to 37.1 kg/m<sup>2</sup>), had not undergone any surgical procedures to their breasts and were not pregnant or currently breastfeeding. Participants had their bra size assessed by a trained bra fitter using best-fit criteria (McGhee and Steele, 2010; White and Scurr, 2012) (mode UK size 34B (range 32A to 38D)), and their chest circumference (median 79 cm, (range 67 to 101 cm)) and bust circumference (median 92 cm, (range 80 to 126 cm)) measurements were recorded.

### **2.2 Laboratory protocol and analysis**

#### **2.2.1 Anthropometrics**

Stretch stature (m) and body mass (kg) measurements were taken to a precision of 10 mm and 0.1 kg respectively, using a Seca free-standing height measure and calibrated Seca scales (Seca, Hamburg, Germany). In accordance with International Society for the Advancement of Kinanthropometry (ISAK) protocols (Marfell-Jones et al., 2012), skinfold measurements were taken at eight sites (triceps, biceps, subscapular, iliac crest, supraspinale, abdominal, front thigh and calf) using Harpenden Skinfold callipers (Baty International, West Sussex, United Kingdom), and waist and hip circumference were

measured using a flexible, steel tape (Lufkin W606PM). Acromiale-radiale length and biacromial breadth (previously investigated in breast anatomy (Cardoso et al., 2015) and bra design research (Chen et al., 2014; Zheng et al., 2007)) were also recorded using a segmometer (Rosscraft) and a large sliding bone calliper (Rosscraft), respectively. Two ISAK trained researchers completed all anthropometric measurements. Both anthropometrists demonstrated high intra-tester reliability producing technical error of measurement for repeated measurements of < 6% for skinfolds and < 2% for all circumferences, breadth, and length measurements. Each measurement was taken twice; with a third measure taken when the technical error of measurement, advised by ISAK (within 7.5% of the first for skinfolds and within 1.5% of the first for remaining measures), was exceeded. The mean skinfold value was calculated where duplicate measurements were recorded, whilst the median skinfold value was utilised where three measurements were recorded (Hume et al., 2017). BMI ( $\text{kg/m}^2$ ) and the sum of eight skinfolds were then calculated for each participant.

### 2.2.2 Breast position

Electromagnetic sensors (240 Hz, Liberty, Polhemus, Vermont, USA) were applied to the centre of the left nipple (LNIP) (Zhou et al., 2011) (with the nipple utilised to represent breast position (Mills et al., 2016)) and torso (suprasternal notch (STN), xiphoid process (XP), 7<sup>th</sup> cervical vertebrae (C7) and 8<sup>th</sup> thoracic vertebrae (T8)) (Wu et al., 2005) to allow for the breast position to be quantified relative to the torso (Figure 1).

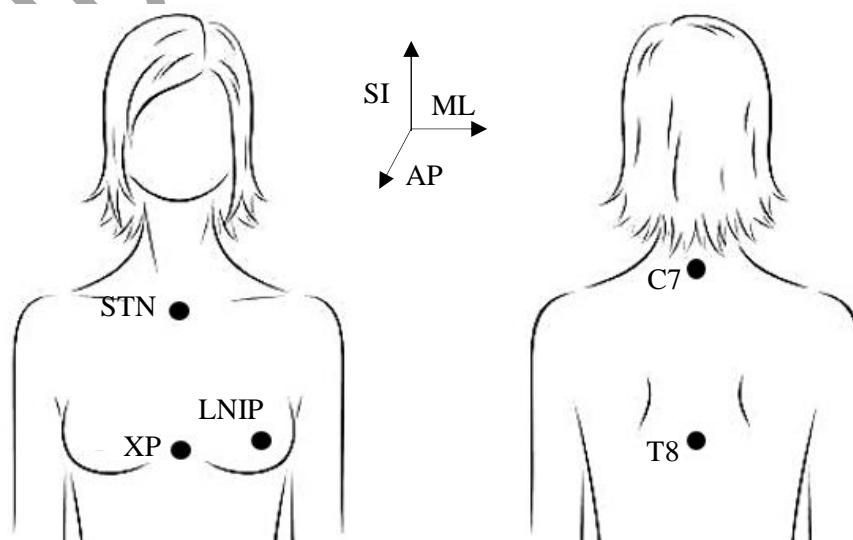


**Figure 1. Local coordinate system (SI, superoinferior; ML mediolateral; AP, anteroposterior) and electromagnetic sensor locations on the left breast and torso.**

Static gravity-loaded sensor coordinates were recorded for 10 s while participants stood in the anatomical position. The neutral breast position was then identified while participants were seated upright, immersed in water (37° C) to the level of their suprasternal notch sensor (Norris et al., 2020). The static positions of the sensors while underwater were recorded for a 10 s trial.

Positional data from the electromagnetic sensors on the breast and torso during standing and water immersion were exported to Visual 3D (v4.96.4, C-motion, Washington DC, USA), and filtered using a generalised cross-validatory quintic spline (Sanchez et al., 2017). A reference torso segment using the 4 torso sensors was created in Visual 3D, to provide a reference co-ordinate system. The proximal end of the torso segment (the origin) was defined using the midpoint between the STN and C7 sensors, and the distal end was defined using the midpoint between the XP and T8 sensors. Mean gravity-loaded and neutral breast positions were then calculated, in all directions, relative to the torso coordinate system.

### **2.3 MRI protocol and analysis**

Prior to the MRI, participants had their bilateral breast boundary identified using the folding line method (Lee et al., 2004). This breast boundary was then outlined with a surgical marker and defined utilising multiple 1000 mg fish-oil capsules attached to the skin. The MRI was then acquired as the participant lay prone, with a breast coil on a Philips Ingenia 1.5 T (Philips Healthcare, Best, Netherlands) using the dual-echo mDixon sequence (software version 5.1.7.2) (Eggers et al., 2011). An acquisition matrix of 300 x 300 was used with in-plane resolution of 1.5 x 1.5 mm<sup>2</sup> and a slice thickness of 3 mm. Anonymised digital imaging and communications in medicine (DICOM) datasets were processed at the Centre for Medical Image Science and Visualization (CMIV) at Linköping University, Sweden. The automated image analysis was performed using AMRA Researcher® (Advanced MR Analytics AB, Linköping, Sweden).

The posterior boundary of the breast segmentation was medially set in the fatty tissue anterior of the pectoral muscle, and laterally by a line crossing the pectoral muscle and sternum. The lateral, medial, superior, and inferior boundaries were defined using the previously attached fish-oil capsules. The following MRI breast variables were then established: bilateral breast volume (cc), breast volume fibroglandular percentage (%), breast volume fat percentage (%), breast fibroglandular mass (kg), breast fat mass (kg), total breast mass (kg) and breast mass-density ( $\text{kg/m}^3$ ). The quantitative fat images were computed by calibrating the original fat images using fatty tissue as an internal intensity reference, thus, allowing fatty tissue volume to be quantified within segmentation (Peterson et al., 2016). The fatty and total breast volumes (cc) were computed based on manual whole-breast segmentation of quantitative water-fat MRI images. Breast volume fibroglandular percentage and breast volume fat percentage were computed as the ratio of fibroglandular and fatty tissue volume to total breast volume respectively (Karlsson et al., 2015). Breast fibroglandular mass, fat mass and total mass were estimated using the MRI composition data, combined with reported mass-density values for both fatty and fibroglandular tissue (Sanchez et al., 2016). Right breast MRI data were then omitted as only left breast position data were collected within the current study (in line with previous studies investigating the neutral breast position (Knight et al., 2014; Mills et al., 2016; Sanchez et al., 2017)).

## **2.4 Statistical analyses**

Data were checked for normality and continuous data that approximated a normal distribution were described using means and standard deviations (SD). Skewed data were described using medians and interquartile ranges (IQR). Shapiro Wilks test was used to determine normality and means/standard deviations, or median/interquartile ranges were presented as appropriate. While descriptive statistics were identified for both breast volume fibroglandular percentage and breast volume fat percentage, due to lack of variable independence, only breast volume fibroglandular percentage was included for further statistical analysis. Breast volume fibroglandular percentage was included due to its association with bra cup size and age (Huang et al., 2011).



Following this, the dependent variable dataset (3 variables) was identified as the neutral breast position variables (anteroposterior, mediolateral and superoinferior) and the full independent variable dataset (17 variables) was identified as the gravity-loaded breast position (in anteroposterior, mediolateral and superoinferior directions), age and anthropometrics (age, BMI, waist-hip ratio, underband circumference, bust circumference, biacromial breadth, acromiale-radiale length and sum of eight skinfolds), and the MRI breast composition variables (breast volume, breast volume fibroglandular percentage, breast fibroglandular mass, breast fat mass, total breast mass and breast mass density). Following this, the simplified independent variable dataset (11 variables) was identified as the full independent variable dataset, minus the MRI breast composition variables (6 variables).

Paired samples t-test was used to identify any significant differences between gravity loaded and neutral breast positions. Pearson's correlation test was used to examine the linear relationship status between dependent and independent variables, with the Pearson's correlation coefficient ( $r$ ) calculated to measure the strength of the associations between the dependent variable dataset and the full independent variable dataset, with associations identified as trivial ( $< 0.3$ ), low ( $\geq 0.3$  and  $< 0.5$ ), moderate ( $\geq 0.5$  and  $< 0.7$ ), high ( $\geq 0.7$  and  $< 0.9$ ) and very high ( $\geq 0.9$ ) (Hinkle et al., 1990). Backwards stepwise multiple linear regression models were then conducted to investigate the effect of the full and simplified independent variable datasets and on each of the dependent variables individually (3D neutral breast position in anteroposterior, mediolateral and superoinferior directions). Additionally, due to the presence of multiple dependent variables multivariate multiple regression was utilised to investigate the effect of the full and simplified independent variable datasets on the combined neutral breast position (representing the 3D neutral breast positions assessed within one model). Each combination of independent variables was investigated to determine the best multivariate multiple regression model, with a maximum of eight independent variables included due to sample size restrictions (Hair et al., 2016). For multivariate multiple regression model selection, the models were then evaluated with respect to having minimum average error (calculated as the Euclidean distance between the observed and model predicted position in the 3D space), and maximum average  $R^2$ . For multiple linear and

multivariate multiple regression analysis the assumption of multicollinearity were assessed based on variance inflation factor (VIF) values, with VIF values  $\leq 5$  deemed acceptable (Rogerson, 2010). Regression equations were identified for all regression models.

Furthermore, to assess model prediction accuracy, where possible (dependent on the predictor variables identified), previously identified (observed) neutral breast positions ( $n = 39$ ; mode UK size 34B, range 32C to 36G, Norris et al., (2020)) will be compared to predicted neutral breast positions (calculated via identified regression equations). Linear regression plots, mean absolute difference (MAD) (m) and root mean square error (RMSE) (m) will be utilised to be quantify accuracy (Piñeiro et al., 2008). A threshold of 5 mm was selected as an acceptable threshold for MAD (Gill, 2015; Hansson et al., 2014). Statistical analysis was undertaken using SPSS Version 24 and R software, with a 5% level of significance used for all statistical tests.

### 3. Results

#### 3.1 Descriptive statistics

Descriptive statistics for the neutral breast position, gravity-loaded breast position, age and anthropometrics and MRI breast composition data illustrated participants with a median age of 25 years (IQR = 11 years), a median breast volume of 635.86 cc (IQR = 468.30 cc) and median total breast mass of 0.61 kg (IQR = 0.43 kg).

**Table 1. Descriptive statistics for the left neutral breast position, gravity-loaded breast position, age and anthropometrics, and MRI breast composition data.**

Category	Variable	Mean (SD)
Neutral breast position	Anteroposterior (m)	0.13 (0.02)
	Mediolateral (m)	0.11 (0.02)
	Superoinferior (m)	-0.18 (0.02)
Gravity-loaded breast position	Anteroposterior (m)	0.13 (0.02)
	Mediolateral (m)	0.11 (0.01)
	Superoinferior (m)	-0.21 (0.02)
Age and anthropometrics	Age <sup>1</sup> (years)	25.0 (11.0)
	BMI <sup>1</sup> (kg/m <sup>2</sup> )	24.1 (4.8)

MRI	Waist-hip ratio <sup>1</sup>	0.74 (0.06)
	Underband circumference <sup>1</sup> (cm)	78.5 (5.3)
	Bust circumference <sup>1</sup> (cm)	91.7 (9.5)
	Biacromial breadth (cm)	37.1 (1.9)
	Acromiale-radiale length (cm)	31.6 (1.9)
	Sum of eight skinfolds (mm)	154.6 (53.9)
	Breast volume <sup>1</sup> (cc)	635.86 (468.30)
	Breast volume fibroglandular percentage <sup>1</sup> (%)	23 (22)
	Breast volume fat percentage <sup>1</sup> (%)	78 (22)
	Breast fibroglandular mass <sup>1</sup> (kg)	0.16 (0.10)
	Breast fat mass <sup>1</sup> (kg)	0.41 (0.44)
	Total breast mass <sup>1</sup> (kg)	0.61 (0.43)
	Breast mass-density <sup>1</sup> (kg/m <sup>3</sup> )	935.33 (34.54)

Note. <sup>1</sup>Skewed data, median (IQR) presented.

### 3.1 Paired t-test

Results from the paired sample t-test identified a statistically significant increase in the position of the breast, as you move from a gravity-loaded breast position to a neutral breast position ( $P < 0.001$  in all directions) (Table 2).

**Table 2. Paired t-test of the gravity-loaded breast position and the neutral breast position.**

Gravity loaded breast position - Neutral breast position	Mean difference (SD)	P
Anteroposterior	-0.004 (0.01)	<0.001
Mediolateral	-0.006 (0.01)	<0.001
Superoinferior	-0.032 (0.02)	<0.001

### 3.2 Associations

For the anteroposterior and the mediolateral neutral breast positions the majority of associations with the independent variables were significant and linearly related (anteroposterior; 77%, 13/17 and mediolateral; 71%, 12/17 (Table 3). However, for the superoinferior neutral breast position, only seven significant, linear relationships with the independent variables were identified (41%), and in general these correlations were weaker than those observed between the independent variables and the anteroposterior and mediolateral neutral breast positions. For example, breast fat mass displayed an  $r$  of 0.78 ( $P < 0.001$ ), 0.62 ( $P < 0.001$ ), and -0.24 ( $P = 0.04$ ) for the anteroposterior, mediolateral and superoinferior neutral breast positions, respectively. The strongest significant associations identified

were the anteroposterior neutral breast position with the anteroposterior gravity-loaded breast position ( $r = 0.90$ ,  $P < 0.001$ ), the anteroposterior neutral breast position with the breast volume ( $r = 0.81$ ,  $P < 0.001$ ), and the mediolateral neutral breast position with the mediolateral gravity-loaded breast position ( $r = 0.81$ ,  $P < 0.001$ ).

**Table 3. Pearson's correlations [r] ( $P$  value) between the dependent variables (individual 3D neutral breast position in anteroposterior, mediolateral and superoinferior directions) and the full independent variable dataset (3D gravity-loaded breast position, age and anthropometrics and MRI breast composition data).**

Category	Variable	Neutral breast position		
		Anteroposterior	Mediolateral	Superoinferior
Gravity- loaded breast position	Anteroposterior	<b>0.90 (&lt;0.001)</b>	<b>0.42 (&lt;0.001)</b>	<b>-0.24 (0.03)</b>
	Mediolateral	<b>0.32 (0.004)</b>	<b>0.81 (&lt;0.001)</b>	-0.10 (0.40)
	Superoinferior	<b>-0.60 (&lt;0.001)</b>	<b>-0.57 (&lt;0.001)</b>	<b>0.62 (&lt;0.001)</b>
Age and anthropometrics	Age	0.03 (0.79)	-0.10 (0.93)	-0.08 (0.49)
	BMI	<b>0.72 (&lt;0.001)</b>	<b>0.55 (&lt;0.001)</b>	-0.16 (0.15)
	Waist-hip ratio	<b>0.26 (0.02)</b>	0.11 (0.33)	0.09 (0.43)
	Underband circumference	<b>0.65 (&lt;0.001)</b>	<b>0.55 (&lt;0.001)</b>	-0.14 (0.23)
	Bust circumference	<b>0.78 (&lt;0.001)</b>	<b>0.61 (&lt;0.001)</b>	-0.21 (0.06)
	Biacromial breadth	0.15 (0.18)	0.11 (0.32)	<b>-0.29 (0.008)</b>
	Acromiale-radiale length	0.02 (0.84)	0.13 (0.25)	<b>-0.32 (0.004)</b>
	Sum of eight skinfolds	<b>0.63 (&lt;0.001)</b>	<b>0.48 (&lt;0.001)</b>	-0.10 (0.40)
MRI	Breast volume	<b>0.81 (&lt;0.001)</b>	<b>0.64 (&lt;0.001)</b>	<b>-0.28 (0.01)</b>
	Breast volume fibroglandular percentage	<b>-0.45 (&lt;0.001)</b>	<b>-0.30 (0.006)</b>	0.04 (0.71)
	Breast fibroglandular mass	0.08 (0.51)	0.07 (0.54)	-0.15 (0.17)
	Breast fat mass	<b>0.78 (&lt;0.001)</b>	<b>0.62 (&lt;0.001)</b>	<b>-0.24 (0.04)</b>
	Total breast mass	<b>0.80 (&lt;0.001)</b>	<b>0.64 (&lt;0.001)</b>	<b>-0.28 (0.01)</b>
	Breast mass-density	<b>-0.45 (&lt;0.001)</b>	<b>-0.30 (0.006)</b>	0.04 (0.71)

*Note.  $P < 0.05$  presented in bold.*

### 3.3. Regression Analysis

VIF values indicated no multicollinearity was present among independent variables (all VIF values  $\leq 5$ ), supported by the majority of correlation coefficients between independent variables identified as trivial, low or moderate ( $r < 0.7$ ) (Appendix 1).

### 3.3.1 Multiple Linear Regression

Three multiple linear regression models were utilised to investigate the relationship between the full independent variable dataset and the dependent variables (individual 3D neutral breast positions) (Table 4). The adjusted  $R^2$  values for the anteroposterior (Model 1), mediolateral (Model 2) and superoinferior (Model 3) neutral breast positions were 0.86, 0.74, and 0.50, respectively.

**Table 4. Multiple linear regression models of the independent 3D neutral breast position in anteroposterior (Model 1), mediolateral (Model 2) and superoinferior (Model 3) directions, with the full independent variable dataset (the gravity-loaded breast position, age and anthropometrics, and MRI breast composition data).**

	$\beta$	SE	<i>P</i>	F-ratio	df	<i>P</i>
<b>Model 1. Anteroposterior neutral breast position</b>						
Anteroposterior gravity-loaded breast position	0.75	0.08	<0.001	142.19	3	<0.001
Biacromial breadth	-0.12	0.00	0.01			
Breast volume	0.23	0.00	0.002			
<b>Model 2. Mediolateral neutral breast position</b>						
Mediolateral gravity-loaded breast position	0.68	0.08	<0.001	57.29	4	<0.001
Superoinferior gravity-loaded breast position	-0.21	0.05	0.003			
Underband circumference	-0.19	0.00	0.007			
Acromiale-radiale length	-0.13	0.00	0.04			
<b>Model 3: Superoinferior neutral breast position</b>						
Anteroposterior gravity-loaded breast position	0.24	0.09	0.02	20.58	4	<0.001
Mediolateral gravity-loaded breast position	0.29	0.10	0.002			
Superoinferior gravity-loaded breast position	0.85	0.07	<0.001			
Acromiale-radiale length	-0.26	0.00	0.002			

Note.  $\beta$ : standardised beta coefficient; SE: standard error; *P*: *p*-value.

The anteroposterior neutral breast position (m) was predicted as  $0.064 + (0.826 \times \text{anteroposterior gravity-loaded breast position}) + (-0.001 \times \text{biacromial breadth}) + (0.000 \times \text{breast volume})$ .

The mediolateral neutral breast position (m) was predicted as  $-0.011 + (0.826 \times \text{mediolateral gravity-loaded breast position}) + (-0.151 \times \text{superoinferior gravity-loaded breast position}) + (0.001 \times \text{underband circumference}) + (-0.001 \times \text{acromiale-radiale length})$ .

The superoinferior neutral breast position (m) was predicted as  $-0.059 + (0.213 \times \text{anteroposterior gravity-loaded breast position}) + (0.307 \times \text{mediolateral gravity-loaded breast position}) + (0.527 \times \text{superoinferior gravity-loaded breast position}) + (-0.002 \times \text{acromiale-radiale length})$ .

Three multiple linear regression models were also utilised to investigate the relationship between the simplified independent variable dataset and the dependent variables (individual 3D neutral breast positions) (Table 5). The adjusted  $R^2$  values for the anteroposterior (Model 1), mediolateral (Model 2) and superoinferior (Model 3) neutral breast positions were 0.83, 0.74, and 0.50, respectively.

**Table 5. Multiple linear regression models for the dependent neutral breast position in all directions, anteroposterior (Model 1), mediolateral (Model 2) and superoinferior (Model 3), with the simplified independent variable dataset (the gravity-loaded breast position, age and anthropometrics).**

	$\beta$	SE	<i>P</i>	F-ratio	df	<i>p</i>
<b>Model 1 Anteroposterior neutral breast position</b>						
Anteroposterior gravity-loaded breast position	0.83	0.08	<0.001	132.41	3	<0.001
BMI	0.15	0.00	0.03			
Biacromial breadth	-0.14	0.00	0.002			
<b>Model 2. Mediolateral neutral breast position</b>						
Mediolateral gravity-loaded breast position	0.68	0.08	<0.001	57.29	4	<0.001
Superoinferior gravity-loaded breast position	-0.21	0.05	0.003			
Underband circumference	0.19	0.00	0.007			
Acromiale-radiale length	-0.13	0.00	0.04			
<b>Model 3: Superoinferior neutral breast position</b>						
Anteroposterior gravity-loaded breast position	0.24	0.09	0.02	20.58	4	<0.001
Mediolateral gravity-loaded breast position	0.29	0.10	0.002			
Superoinferior gravity-loaded breast position	0.85	0.07	<0.001			

Acromiale-radiale length	-0.26	0.00	0.002
--------------------------	-------	------	-------

Note.  $\beta$ : standardised beta coefficient; SE: standard error; P: p-value.

The anteroposterior neutral breast position (m) was predicted as  $0.050 + (0.912 \times \text{anteroposterior gravity-loaded breast position}) + (0.001 \times \text{BMI}) + (-0.001 \times \text{biacromial breadth})$ .

The mediolateral neutral breast position (m) was predicted as  $-0.011 + (0.826 \times \text{mediolateral gravity-loaded breast position}) + (-0.151 \times \text{superoinferior gravity-loaded breast position}) + (0.001 \times \text{underband circumference}) + (-0.001 \times \text{acromiale-radiale length})$ .

The superoinferior neutral breast position (m) was predicted as  $-0.059 + (0.213 \times \text{anteroposterior gravity-loaded breast position}) + (0.307 \times \text{mediolateral gravity-loaded breast position}) + (0.527 \times \text{superoinferior gravity-loaded breast position}) + (-0.002 \times \text{acromiale-radiale length})$ .

### 3.3.2 Multivariate Multiple Regression

Within the multivariate multiple regression analysis (utilised to predict the combined neutral breast position), model iterations were evaluated with respect to having minimum average error (calculated as the Euclidean distance between the observed and model predicted 3D position), and maximum average adjusted  $R^2$ . While multivariate multiple regression analysis was performed for both the full and simplified independent variable datasets, both analyses resulted in the same model with the shortest average error, with this model including only the anteroposterior gravity-loaded breast position and the mediolateral gravity-loaded breast position as independent variables (Table 6). The average adjusted  $R^2$  values for this multivariate multiple regression were 0.81, 0.69 and 0.03 for the anteroposterior, mediolateral and superoinferior positions, respectively. Additionally, the top ten multivariate multiple regression models for both the full and simplified independent variable datasets were identified and presented based on these performance metrics (Appendix 2 and 3).

Variable	$\beta$	SE	P	F	df	p
----------	---------	----	---	---	----	---

<b>Anteroposterior</b>						
Anteroposterior gravity-loaded breast position	0.96	0.06	<0.001	174.60	2	<0.001
Mediolateral gravity-loaded breast position	0.12	0.07	0.08			
<b>Mediolateral</b>						
Anteroposterior gravity-loaded breast position	0.23	0.07	<0.001	89.70	2	<0.001
Mediolateral gravity-loaded breast position	0.91	0.08	<0.001			
<b>Superoinferior</b>						
Anteroposterior gravity-loaded breast position	-0.20	0.10	0.05	2.341	2	0.10
Mediolateral gravity-loaded breast position	-0.04	0.12	0.76			

**Table 6. Multivariate multiple regression for the combined neutral breast position.**

*Note. B: standardised beta coefficient; SE: standard error; P: p-value.*

The anteroposterior neutral breast position (m) was predicted as  $-0.004 + (0.961 \times \text{anteroposterior gravity-loaded breast position}) + (0.119 \times \text{mediolateral gravity-loaded breast position})$ .

The mediolateral neutral breast position (m) was predicted as  $-0.014 + (0.228 \times \text{anteroposterior gravity-loaded breast position}) + (0.911 \times \text{mediolateral gravity-loaded breast position})$ .

The superoinferior neutral breast position (m) was predicted as  $-0.148 + (-0.199 \times \text{anteroposterior gravity-loaded breast position}) + (-0.038 \times \text{mediolateral gravity-loaded breast position})$ .

### 3.3.3 Evaluating model prediction accuracy

Following on from the regression analysis, the multivariate multiple linear regression models were then assessed for accuracy (Figure 2).  $R^2$  values of 0.82, 0.45 and 0.16, MAD values of 0.006 m, 0.009 m and 0.015 m, and RMSE values of 0.007 m, 0.013 m and 0.018 m were identified for the anteroposterior, mediolateral and superoinferior neutral breast positions, respectively. All MAD values were  $> 0.005$  m and therefore multivariate model prediction was identified as inaccurate.



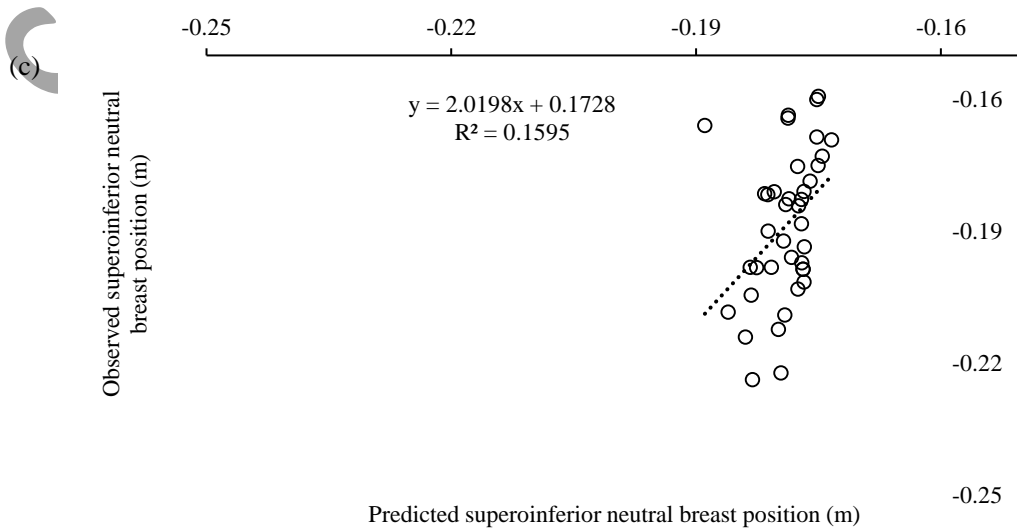
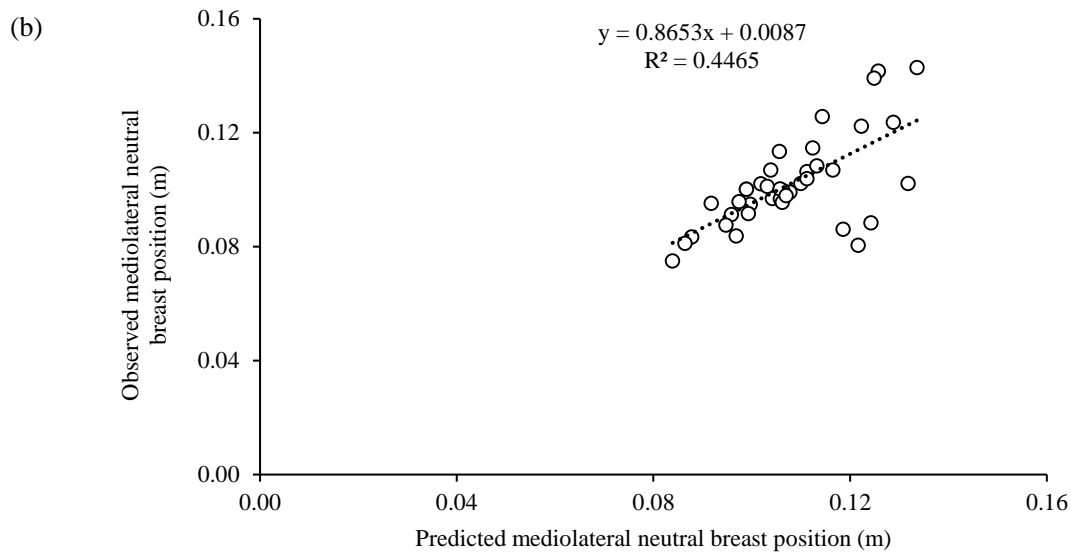
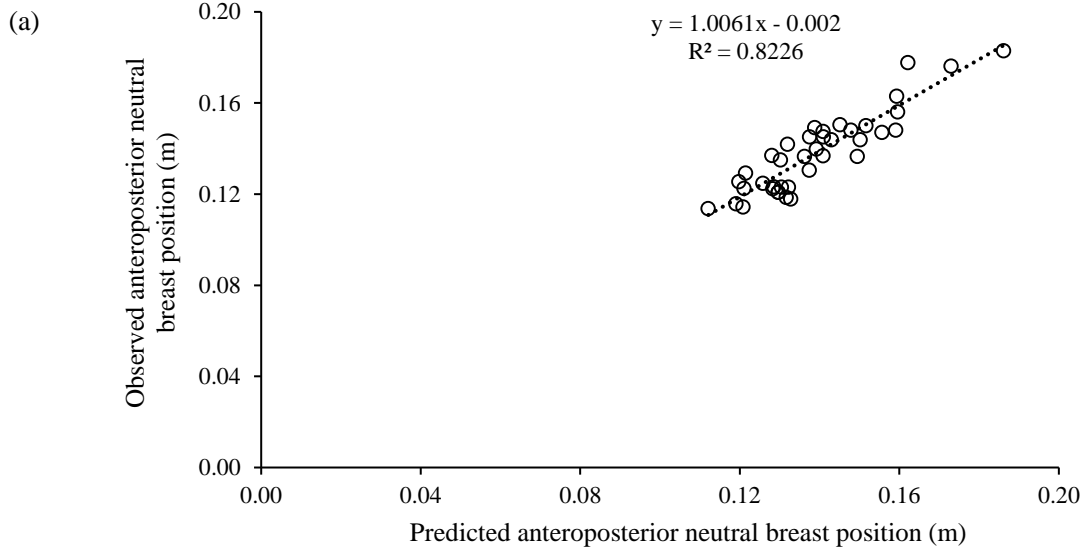


**Figure 2. Observed (Norris et al., 2020) versus predicted neutral breast position (m) linear regression plots, in the (a) anteroposterior, (b) mediolateral and (c) superoinferior direction.**

#### **4. Discussion**

This study firstly aimed to utilise regression modelling to identify the predictor variables which account for neutral breast position variance, using a full independent variable dataset, and a simplified independent variable dataset. Based on the predictive models conducted, 3% to 86% of variance in the neutral breast position was accounted for by the gravity-loaded breast position (in all directions), anthropometrics (BMI, biacromial breadth, underband circumference and acromial-radial length) and MRI breast composition data (breast volume). This study then aimed to assess model prediction accuracy, with a threshold of 5 mm. When utilising multivariate multiple regression modelling, the gravity loaded breast position alone (anteroposterior and mediolateral gravity-loaded breast positions) predicted the neutral breast positions to within 6 mm, when compared to previously identified neutral breast positions (Norris et al., 2020), and therefore did not accurately predict the neutral breast position.

In general, the anteroposterior and mediolateral neutral breast positions displayed stronger correlations with the independent variables, than the superoinferior neutral breast position. The superoinferior breast position may be more impacted by the mechanical properties of the breast supporting structures than the anteroposterior and mediolateral breast positions. Within the current study, the mechanical properties of the Coopers ligaments and breast skin were not investigated, and it is therefore possible that these variables may contributed to the change in superoinferior breast position not currently explained. Additionally, Mills et al., (2016) identified that the breast moves superiorly when immersed in water, compared to when gravity-loaded. While this was observed in the current study, Mills et al., (2016) also suggested that the range of breast densities observed in a group of females may mean that breast immersion in water (which has a uniform density) is unlikely to replicate the neutral breast position for every female. This was supported by the findings from Mills et al., (2016) who reported significant differences in the superoinferior nipple position, between immersion in water and soybean oil (which is denser than water). Within the current study, the use of water for neutral breast position

estimation, may have resulted in weaker relationships occurring with the superoinferior neutral breast position. Breast volume fibroglandular percentages for participants within the current study fell in multiple BI-RADS breast density categories, category 1 (<25% breast volume fibroglandular percentage, 42 participants), 2 (25% to 50% breast volume fibroglandular percentage, 27 participants) and 3 (51% to 75% breast volume fibroglandular percentage, 11 participants) (Gweon et al., 2013), with this variation in breast density possibly not replicated by water immersion alone. However, water alone has been previously utilised (Rajagopal et al., 2008), and shown to produce acceptable estimates of the neutral breast position (within 5.6 mm) (Mills et al., 2016).

When investigating potential predictors of the neutral breast position, breast volume was the only MRI breast composition variable to contribute, and this was solely in the anteroposterior direction. This contribution was possibly unnecessary however, as while 86% of the variance in the anteroposterior neutral breast position was accounted for when utilising the full independent dataset, this only decreased to 83% when utilising the simplified independent dataset. Additionally, when utilising the simplified independent variable dataset 74% of the variance in the mediolateral neutral breast position was accounted for, along with 50% of the variance in the superoinferior direction. The amount of variance accounted for within the multiple regression models conducted within this study, on individual 3D neutral breast positions (50% to 86%), were higher than that identified by Coltman et al., (2018) when predicting upper torso musculoskeletal pain from breast characteristics (23%), and similar to that identified by Koch et al., (2011) when predicting breast volume (59% to 77%). However, when multivariate multiple linear regression was utilised to predict the combined neutral position, less variance was accounted for (3% to 81%). Given the complexity of MRI breast composition data collection and its marginal contribution to neutral breast position prediction, the current study suggests that it is unnecessary for this application.

The gravity-loaded breast position was identified as a predictor in both the neutral breast position when assessed in each 3D direction individually, and the combined neutral breast position. Additionally, the anthropometric measures BMI, biacromial breadth, underband circumference and acromiale-radiale

length were all included as significant predictors of the neutral breast position when assessed in each 3D direction individually. BMI, along with sternal notch to nipple distance, has previously been identified to contribute to half the variance in breast mass (Brown et al., 2012), with current results further supporting Brown et al., (2012) suggestion that body composition (although possibly not breast composition) may affect breast support requirements. In regards to biacromial breadth and underband circumference, the results of the current study compliments work by Zheng et al., (2007), who identified circumference variables (body build indices such as BMI, body width and depth variables) as Factor 1 when utilising Principal Component Analysis (PCA) to identify anthropometric variables which best describe body shape. When combined with the current results, this may further support the role of anthropometrics in describing, and in fact predicting breast characteristics such as shape and position.

When assessing model prediction accuracy, predicted anteroposterior, mediolateral and superoinferior neutral breast positions were all  $> 5$  mm different from previously identified neutral breast positions, indicating that the gravity-loaded anteroposterior and mediolateral breast positions alone, do not accurately predict the neutral breast position. If integrated into the bra design and development process, imprecise breast positioning may contribute to the development of poorly designed bras, which when added to the bra market may cause consumer dissatisfaction (Chen et al., 2011). While Chan et al., (2001) suggested that continual innovation should occur, and improvements should be made within the bra industry to improve bra development and performance, further work is required within this innovative research to identify additional variables which accurately predict the neutral breast position to within 5 mm.

While this is the first study to investigate predicting the neutral breast position, it is not without limitations. Firstly, while we identified an extensive selection of biomechanical and physiological variables as potential neutral breast position predictors, it is possible further predictors exist. For example, when developing a new Chinese bra sizing system Zheng et al., (2007) identified 98 breast characteristics which described breast shape utilising 3D body scanning. While Zheng et al., (2007) 98 breast characteristics may aid in the prediction of the neutral breast position, this study focused on the

collection of a number of simple variables (excluding MRI breast composition data), to increase the feasibility of neutral breast position integration within the bra industry.

## **5. Conclusion**

The current study identified that MRI breast composition data only marginally contributed to neutral breast position prediction, with only breast volume identified as a predictor of the anteroposterior neutral breast position. Additionally, when predicting the combined neutral breast position, while the gravity-loaded breast position alone (anteroposterior, and mediolateral) accounted for 81% and 69% of the variance in the anteroposterior and mediolateral neutral breast positions, 97% of the variance in the superoinferior neutral breast position remains unexplained. Lastly, the gravity-loaded breast position alone does not accurately predict the neutral breast position ( $MAD > 5$  mm in all directions), when compared to observed neutral breast positions. Prior to implementation in bra development, further work is required to identify additional variables which successfully predict the neutral breast position.

## **6. Acknowledgements**

We thank Brogan Jones, Melissa Jones, Caitlyn Hamilton and Anna Marczyk for assistance during data collection.

## **7. Funding**

This work was supported, in part, by Science Foundation Ireland grant 13/RC/2094 and has received funding from the European Union's Horizon 2020 research and innovation programme under the Marie Skłodowska-Curie grant agreement No 754489. M. Norris and A. Sanchez also received funding for the current study from Hanes Brands Inc., whilst T. Blackmore received funding for the current study from Adidas AG. For the remaining authors none were declared.

## **References**

Bridgman, C., Scurr, J., White, J., Hedger, W., Galbraith, H., 2010. Three-dimensional kinematics of

- the breast during a two-step star jump. *J. Appl. Biomech.* 26, 465–472.  
<https://doi.org/10.1123/jab.26.4.465>
- Brown, N., White, J., Milligan, A., Risius, D., Ayres, B., Hedger, W., Scurr, J., 2012. The relationship between breast size and anthropometric characteristics. *Am. J. Hum. Biol.* 24, 158–164.  
<https://doi.org/10.1002/ajhb.22212>
- Cardoso, A., Santos, D., Martins, J., Coelho, G., Barroso, L., Costa, H., 2015. Breast ligaments: an anatomical study. *Eur. J. Plast. Surg.* 38, 91–96. <https://doi.org/10.1007/s00238-014-1024-7>
- Caruso, M.K., Guillot, T.S., Nguyen, T., Greenway, F.L., 2006. The cost effectiveness of three different measures of breast volume. *Aesthetic Plast. Surg.* 30, 16–20. <https://doi.org/10.1007/s00266-004-0105-6>
- Chan, C.Y.C., Yu, W.W.M., Newton, E., 2001. Evaluation and analysis of bra design. *Des. J.* 4, 33–40.  
<https://doi.org/10.2752/146069201789389601>
- Chen, C.-M., LaBat, K., Bye, E., 2011. Bust prominence related to bra fit problems. *Int. J. Consum. Stud.* 35, 695–701. <https://doi.org/10.1111/j.1470-6431.2010.00984.x>
- Chen, Yuexing, Ying, B., Zhang, X., Chen, Yilin, 2014. Characteristic parameters analysis on breast shape for moulded bra cup and bra structure design. *J. Fiber Bioeng. Informatics* 7, 429–439.  
<https://doi.org/10.3993/jfbi09201412>
- Coltman, C.E., Steele, J.R., McGhee, D.E., 2018. Can breast characteristics predict upper torso musculoskeletal pain? *Clin. Biomech.* 53, 46–53.  
<https://doi.org/10.1016/j.clinbiomech.2018.02.002>
- Eggers, H., Brendel, B., Duijndam, A., Herigault, G., 2011. Dual-echo Dixon imaging with flexible choice of echo times. *Magn. Reson. Med.* 65, 96–107. <https://doi.org/10.1002/mrm.22578>
- Fowler, P.A., Casey, C.E., Cameron, G.G., Foster, M.A., Knight, C.H., 1990. Cyclic changes in composition and volume of the breast during the menstrual cycle, measured by magnetic resonance imaging. *BJOG An Int. J. Obstet. Gynaecol.* 97, 595–602.  
<https://doi.org/10.1111/j.1471-0528.1990.tb02546.x>
- Georgiade, N.G., Georgiade, G.S., Riefkohl, R., 1990. *Aesthetic surgery of the breast*. Springer.
- Gill, S., 2015. A review of research and innovation in garment sizing, prototyping and fitting. *Text.*

504 Prog. 47, 1–85. <https://doi.org/10.1080/00405167.2015.1023512>

505 Graham, S.J., Bronskill, M.J., Byng, J.W., Yaffe, M.J., Boyd, N.F., 1996. Quantitative correlation of

506 breast tissue parameters using magnetic resonance and X-ray mammography. *Br. J. Cancer* 73,

507 162–168. <https://doi.org/10.1038/bjc.1996.30>

508 Gweon, H.M., Youk, J.H., Kim, J.-A., Son, E.J., 2013. Radiologist assessment of breast density by BI-

509 RADS categories versus fully automated volumetric assessment. *Am. J. Roentgenol.* 201, 692–

510 697. <https://doi.org/10.2214/AJR.12.10197>.

511 Hair, J., Anderson, R., Black, B., Babin, B., 2016. Multivariate data analysis. Pearson Education.

512 Halinski, R.S., Feldt, L.S., 1970. The selection of variables in multiple regression analysis. *J. Educ.*

513 *Meas.* 7, 151–157. <https://doi.org/10.1111/j.1745-3984.1970.tb00709.x>

514 Hansson, E., Manjer, J., Ringberg, A., 2014. Inter-observer reliability of clinical measurement of

515 suprasternal notch-nipple distance and breast ptosis. *Indian J. Plast. Surg. Off. Publ. Assoc. Plast.*

516 *Surg. India* 47, 61–64. <https://doi.org/10.4103/0970-0358.129625>

517 Herold, C., Reichelt, A., Stieglitz, L.H., Dettmer, S., Knobloch, K., Lotz, J., Vogt, P.M., 2010. MRI-

518 based breast volumetry-evaluation of three different software solutions. *J. Digit. Imaging* 23, 603–

519 610. <https://doi.org/10.1007/s10278-009-9264-y>

520 Hinkle, D.E., Wiersma, W., Jurs, S.G., 1990. Applied statistics for the behavioral sciences. Houghton

521 Mifflin. <https://doi.org/10.2307/1164825>

522 Huang, S.Y., Boone, J.M., Yang, K., Packard, N.J., McKenney, S.E., Prionas, N.D., Lindfors, K.K.,

523 Yaffe, M.J., 2011. The characterization of breast anatomical metrics using dedicated breast CT.

524 *Med. Phys.* 38, 2180–2191. <https://doi.org/10.1118/1.3567147>

525 Hume, P.A., Kerr, D.A., Ackland, T.R., 2017. Best practice protocols for physique assessment in sport,

526 Springer. <https://doi.org/10.1007/978-981-10-5418-1>

527 Karlsson, A., Rosander, J., Romu, T., Tallberg, J., Grönqvist, A., Borga, M., Dahlqvist Leinhard, O.,

528 2015. Automatic and quantitative assessment of regional muscle volume by multi-atlas

529 segmentation using whole-body water–fat MRI. *J. Magn. Reson. Imaging* 41, 1558–1569.

530 <https://doi.org/10.1002/jmri.24726>

531 Klifa, C., Carballido-Gamio, J., Wilmes, L., Laprie, A., Shepherd, J., Gibbs, J., Fan, B., Noworolski,

S., Hylton, N., 2010. Magnetic resonance imaging for secondary assessment of breast density in a high-risk cohort. *Magn. Reson. Imaging* 28, 8–15. <https://doi.org/10.1016/j.mri.2009.05.040>

Knight, M., Wheat, J., Driscoll, H., Haake, S., 2014. A novel method to find the neutral position of the breast. *Procedia Eng.* 72, 20–25. <https://doi.org/10.1016/j.proeng.2014.06.007>

Koch, M.C., Adamietz, B., Jud, S.M., Fasching, P.A., Haeberle, L., Karbacher, S., Veit, K., Schulz-Wendtland, R., Uder, M., Beckmann, M.W., Bani, M.R., Heusinger, K., Loehberg, C.R., Cavallaro, A., 2011. Breast volumetry using a three-dimensional surface assessment technique. *Aesthetic Plast. Surg.* 35, 847–855. <https://doi.org/10.1007/s00266-011-9708-x>

Lee, H.-Y.H.Y.H.-Y., Hong, K., Kim, E.A., Ae, E., 2004. Measurement protocol of women's nude breasts using a 3D scanning technique. *Appl. Ergon.* 35, 353–359. <https://doi.org/10.1016/j.apergo.2004.03.004>

McCann, J. and Bryson, D., (2014). *Textile led design for the active ageing population*. Woodhead Publishing. ISBN-13: 9780857098788; ISBN-10: 0857098780.

McGhee, D.E., Steele, J.R., 2020. Breast biomechanics: What do we really know? *Physiology* 35, 144–156. <https://doi.org/10.1152/physiol.00024.2019>

McGhee, D.E., Steele, J.R., 2010. Optimising breast support in female patients through correct bra fit. A cross-sectional study. *J Sci Med Sport* 13, 568–572. <https://doi.org/10.1016/j.jsams.2010.03.003>

McGhee, D.E., Steele, J.R., Zealey, W.J., Takacs, G.J., 2013. Bra-breast forces generated in women with large breasts while standing and during treadmill running: Implications for sports bra design. *Appl Erg.* 44, 112–118. <https://doi.org/10.1016/j.apergo.2012.05.006>

Milligan, A., Mills, C., Corbett, J., Scurr, J., 2015a. The influence of breast support on torso, pelvis and arm kinematics during a five kilometer treadmill run. *Hum. Mov. Sci.* 42, 246–260. <https://doi.org/10.1016/j.humov.2015.05.008>

Milligan, A., Mills, C., Corbett, J., Scurr, J., 2015b. Magnitude of multiplanar breast kinematics differs depending upon run distance. *J. Sports Sci.* 33, 2025–2034. <https://doi.org/10.1080/02640414.2015.1026376>

Mills, C., Ayres, B., Scurr, J., 2015. Breast support garments are ineffective at reducing breast motion



during an aqua aerobics jumping exercise. *J. Hum. Kinet.* 46, 49–58.  
<https://doi.org/10.1515/hukin-2015-0033>

Mills, C., Sanchez, A., Scurr, J., 2016. Estimating the gravity induced three dimensional deformation of the breast. *J. Biomech.* 49, 4134–4137. <https://doi.org/10.1016/j.jbiomech.2016.10.012>

Nie, K., Chen, J.J.H., Chan, S., Chau, M.M.K.I., Yu, H.J., Bahri, S., Tseng, T., Nalcioğlu, O., Su, M.Y., 2008. Development of a quantitative method for analysis of breast density based on three-dimensional breast MRI. *Med. Phys.* 35, 5253–5262. <https://doi.org/10.1118/1.3002306>

Norris, M., Mills, C., Sanchez, A., Wakefield-Scurr, J., 2020. Do static and dynamic activities induce potentially damaging breast skin strain? *BMJ Open Sp Ex Med* 6, 770. <https://doi.org/10.1136/bmjsem-2020-000770>

Norris, M., Sanchez, A., Mills, C., Wakefield-Scurr, J., 2018. Breast skin strain during everyday activities, in: 8th World Congress of Biomechanics. Dublin. <https://doi.org/10.13140/RG.2.2.35978.36807>

Peterson, P., Romu, T., Brorson, H., Dahlqvist Leinhard, O. Månsson, S., 2016. Fat quantification in skeletal muscle using multigradient-echo imaging: Comparison of fat and water references. *J. Magn. Reson. Imaging* 43, 203–212. <https://doi.org/10.1002/jmri.24972>

Piñeiro, G., Perelman, S., Guerschman, J.P., Paruelo, J.M., 2008. How to evaluate models: Observed vs. predicted or predicted vs. observed? *Ecol. Modell.* 216, 316–322. <https://doi.org/10.1016/j.ecolmodel.2008.05.006>

Rajagopal, V., Lee, A., Chung, J.-H., Warren, R., Highnam, R.P., Nash, M.P., Nielsen, P.M.F., 2008. Creating individual-specific biomechanical models of the breast for medical image analysis. *Acad. Radiol.* 15, 1425–36. <https://doi.org/10.1016/j.acra.2008.07.017>

Regnault, P., 1976. Breast ptosis. Definition and treatment. *Clin. Plast. Surg.* 3, 193–203.

Rinker, B., Veneracion, M., Walsh, C.P., 2010. Breast ptosis: Causes and cure. *Ann. Plast. Surg.* 64, 579–584. <https://doi.org/10.1097/SAP.0b013e3181c39377>

Risius, D., Milligan, A., Mills, C., Scurr, J., 2015. Multiplanar breast kinematics during different exercise modalities. *Eur. J. Sport Sci.* 15, 111–117. <https://doi.org/10.1080/17461391.2014.928914>

- Rogerson, P.A., 2010. Statistical Methods for Geography. A Student's Guide.
- Rigby and Pellar. 2022. *Exclusive 3D Technology*. Available at: <https://www.rigbyandpeller.com/en-gb/3d-mirror> (Accessed 17<sup>th</sup> August 2022).
- Sak, M.A., Littrup, P.J., Duric, N., Mullooly, M., Sherman, M.E., Gierach, G.L., 2015. Current and future methods for measuring breast density: a brief comparative review. *Breast Cancer Manag.* 4, 209–221. <https://doi.org/10.2217/bmt.15.13>
- Sanchez, A., 2015. Breast skin strain during gravitational and dynamic loading. University of Portsmouth.
- Sanchez, A., Mills, C., Haake, S., Norris, M., Scurr, J., Sanchez, A., 2017. Quantification of gravity-induced skin strain across the breast surface. *Clin. Biomech.* 50, 47–55. <https://doi.org/10.1016/j.clinbiomech.2017.10.005>
- Sanchez, A., Mills, C., Scurr, J., 2016. Estimating breast mass-density: a retrospective analysis of radiological data. *Breast J.* 23, 237–239. <https://doi.org/10.1111/tbj.12725>
- Scurr, J., White, J., Hedger, W., 2010. The effect of breast support on the kinematics of the breast during the running gait cycle. *J. Sports Sci.* 28, 1103–1109. <https://doi.org/10.1080/02640414.2010.497542>
- Silver, F.H.F., Freeman, J.W., Devore, D., 2001. Viscoelastic properties of human skin and processed dermis. *Ski. Res. Technol.* 7, 18–23. <https://doi.org/10.1034/j.1600-0846.2001.007001018.x>
- Wang, C., Wang, L., Kuo, L., Su, F., 2017. Comparison of breast motion at different levels of support during physical activity. *J. Hum. Sport Exerc.* 12, 1256–1264. <https://doi.org/10.14198/jhse.2017.124.12>
- White, J., Scurr, J., 2012. Evaluation of professional bra fitting criteria for bra selection and fitting in the UK. *Ergonomics* 55, 704–711. <https://doi.org/10.1080/00140139.2011.647096>
- Wu, G.G., van der Helm, F.C.T.T., Veeger, H.E.J.D., Makhsous, M., Van Roy, P., Anglin, C., Nagels, J., Karduna, A.R., McQuade, K., Wang, X., Werner, F.W., Buchholz, B., (DirkJan) Veeger, H.E.J., Makhsous, M., Van Roy, P., Anglin, C., Nagels, J., Karduna, A.R., McQuade, K., Wang, X., Werner, F.W., Buchholz, B., Veeger, H.E.J.D., Makhsous, M., Van Roy, P., Anglin, C., Nagels, J., Karduna, A.R., McQuade, K., Wang, X., Werner, F.W., Buchholz, B., (DirkJan)

- Veeger, H.E.J., Makhsous, M., Van Roy, P., Anglin, C., Nagels, J., Karduna, A.R., McQuade, K., Wang, X., Werner, F.W., Buchholz, B., Veeger, H.E.J.D., Makhsous, M., Van Roy, P., Anglin, C., Nagels, J., Karduna, A.R., McQuade, K., Wang, X., 2005. ISB recommendation on definitions of joint coordinate systems of various joints for the reporting of human joint motion—Part II: shoulder, elbow, wrist and hand. *J. Biomech.* 38, 981–992. <https://doi.org/10.1016/j.jbiomech.2004.05.042>
- Zheng, R., Yu, W., Fan, J., 2007. Development of a new chinese bra sizing system based on breast anthropometric measurements. *Int. J. Ind. Ergon.* 37, 697–705. <https://doi.org/10.1016/j.ergon.2007.05.008>
- Zhou, J., Yu, W., Ng, S.-P., 2011. Methods of studying breast motion in sports bras: a review. *Text. Res. J.* 81, 1234–1248. <https://doi.org/10.1177/0040517511399959>
- Zhou, J., Yu, W., Ng, S., 2013. Identifying effective design features of commercial sports bras. *Text. Res. J.* 83, 1500–1513. <https://doi.org/10.1177/0040517512464289>
- Zolfagharnasab, H., Bessa, S., Oliveira, S.P., Faria, P., Teixeira, J.F., Cardoso, J.S., Oliveira, H.P., 2018. A regression model for predicting shape deformation after breast conserving surgery. *Sensors (Switzerland)* 18, 167. <https://doi.org/10.3390/s18010167>

# Appendix 1. Pearson's correlation coefficient (r) values for all independent variables.

Independent Variables	Gravity loaded breast position (anteroposterior)	Gravity loaded breast position (mediolateral)	Gravity loaded breast position (superoinferior)	Age	BMI	Waist-hip ratio	Underband circumference	Bust circumference	Biacromial breadth	Acromiale-radiale length	Sum of eight skinfolds	Breast volume	Breast volume FG percentage	Breast FG mass	Breast fat mass	Total breast mass	Breast mass-density
Gravity loaded breast position (anteroposterior)	1																
Gravity loaded breast position (mediolateral)	0.26*	1															
Gravity loaded breast position (superoinferior)	-0.62***	-0.44***	1														
Age	0.06	-0.06	-0.08	1													
BMI	<b>0.72***</b>	0.38**	-0.57***	0.06	1												
Waist-hip ratio	0.20	0.07	-0.05	-0.15	0.28*	1											
Underband circumference	<b>0.70***</b>	0.40***	-0.47***	0.13	<b>0.81***</b>	0.38***	1										
Bust circumference	<b>0.80***</b>	0.49***	-0.60***	0.08	<b>0.85***</b>	0.32**	<b>0.82***</b>	1									
Biacromial breadth	0.30**	0.01	-0.33**	-0.07	0.24*	0.13	0.18	0.28*	1								
Acromiale-radiale length	0.11	0.30**	-0.20	0.08	-0.09	-0.15	0.06	0.10	0.37**	1							
Sum of eight skinfolds	0.62***	0.40***	-0.48***	0.02	<b>0.82***</b>	0.24*	0.61***	<b>0.70***</b>	0.04	-0.03	1						
Breast volume	<b>0.79***</b>	0.54***	<b>-0.74***</b>	-0.08	<b>0.75***</b>	0.18	0.63***	<b>0.83***</b>	0.18	0.08	<b>0.73***</b>	1					
Breast volume FG percentage	-0.44***	-0.21	0.39***	-0.20	-0.65***	-0.21	-0.59***	-0.57***	-0.04	0.17	<b>-0.71***</b>	-0.53***	1				
Breast FG mass	0.05	0.17	-0.12	-0.26*	-0.32	-0.19	-0.32**	-0.12	0.02	0.20	-0.23*	0.11	0.69***	1			
Breast fat mass	<b>0.77***</b>	0.49***	<b>-0.71***</b>	-0.01	<b>0.81***</b>	0.23*	<b>0.71***</b>	<b>0.86***</b>	0.17	0.03	<b>0.79***</b>	<b>0.97***</b>	<b>-0.70***</b>	-0.14	1		
Total breast mass	<b>0.79***</b>	0.54***	<b>-0.74***</b>	-0.09	<b>0.74***</b>	0.18	0.61***	<b>0.82***</b>	0.18	0.09	<b>0.71***</b>	<b>0.99***</b>	-0.49***	0.16	<b>0.96***</b>	1	
LB mass-density	-0.44***	-0.21	0.39***	-0.20	-0.65***	-0.21	-0.59***	-0.57***	-0.04	0.17	<b>-0.71***</b>	-0.53***	1.0***	0.69***	-0.70***	-0.49***	1

Note. High ( $\geq 0.7$  and  $< 0.9$ ) and very high ( $\geq 0.9$ ) correlations represented in bold. \*  $P < 0.05$ , \*\*  $P < 0.01$  and \*\*\*  $P < 0.001$ . FG: fibroglandular.

**Appendix 2. Model selection statistics for the top ten performing multivariate multiple regression models utilising the full independent variable dataset.**

Performance	Variables included	Average error <sup>†</sup>	Adjusted R <sup>2</sup>	Average adjusted R <sup>2</sup>
1	Anteroposterior gravity-loaded breast position, mediolateral gravity-loaded breast position.	0.017	X:0.81 Y:0.69 Z:0.03	0.51
2	Age, sum of eight skinfolds, breast volume, breast volume fibroglandular percentage, breast fibroglandular mass, breast fat mass.	0.021	X:0.64 Y:0.37 Z:0.07	0.36
3	BMI, breast volume, breast volume fibroglandular percentage, breast fat mass.	0.021	X:0.67 Y:0.40 Z:0.05	0.37
4	BMI, breast volume, breast volume fibroglandular percentage.	0.021	X:0.67 Y:0.40 Z:0.07	0.38
5	BMI, breast volume, breast volume fibroglandular percentage, breast fat mass, breast mass-density.	0.021	X:0.67 Y:0.40 Z:0.05	0.41
6	Waist-hip ratio, sum of eight skinfolds, breast volume, breast volume fibroglandular percentage, breast fibroglandular mass, breast fat mass, total breast mass, breast mass-density.	0.021	X:0.64 Y:0.36 Z:0.05	0.35
7	BMI, bust circumference, acromiale-radiale length, breast fibroglandular mass.	0.021	X:0.64 Y:0.37 Z:0.11	0.37
8	Age, sum of eight skinfolds, breast volume, breast fibroglandular mass, breast volume fibroglandular percentage, breast mass-density.	0.021	X:0.64 Y:0.37 Z:0.07	0.37
9	Age, sum of eight skinfolds, breast volume, breast volume fibroglandular percentage, breast fibroglandular mass, breast mass-density.	0.021	X:0.64 Y:0.37 Z:0.07	0.36
10	BMI, breast volume, breast volume fibroglandular percentage, breast mass-density.	0.021	X:0.67 Y:0.40 Z:0.05	0.37

Note. <sup>†</sup>calculated as the Euclidean distance between the observed and model predicted position in the three-dimensional space.

**Appendix 3. Model selection statistics for the top ten performing multivariate multiple regression models utilising the simplified independent variable dataset.**

Performance	Variables included	Average error <sup>†</sup>	Adjusted R <sup>2</sup>	Average adjusted R <sup>2</sup>
1	Anteroposterior gravity-loaded breast position, mediolateral gravity-loaded breast position.	0.017	X:0.81 Y:0.69 Z:0.03	0.51
2	BMI, waist-hip ratio, underband circumference, bust circumference, biacromial breadth, acromiale-radiale length.	0.021	X:0.59 Y:0.35 Z:0.11	0.35
3	Age, BMI, underband circumference, bust circumference, biacromial breadth, acromiale-radiale length, sum of eight skinfolds.	0.021	X:0.59 Y:0.34 Z:0.09	0.34
4	Age, waist-hip ratio, bust circumference, biacromial breadth, acromiale-radiale length, sum of eight skinfolds.	0.021	X:0.59 Y:0.35 Z:0.11	0.35
5	Age, BMI, waist-hip ratio, underband circumference, bust circumference, biacromial breadth, acromiale-radiale length.	0.021	X:0.59 Y:0.35 Z:0.10	0.35
6	BMI, underband circumference, bust circumference, biacromial breadth, acromiale-radiale length, sum of eight skinfolds.	0.021	X:0.59 Y:0.34 Z:0.10	0.34
7	Waist-hip ratio, bust circumference, biacromial breadth, acromiale-radiale length, sum of eight skinfolds.	0.021	X:0.59 Y:0.35 Z:0.12	0.35
8	Age, BMI, waist-hip ratio, bust circumference, biacromial breadth, acromiale-radiale length, sum of eight skinfolds.	0.021	X:0.59 Y:0.35 Z:0.10	0.35
9	Age, waist-hip ratio, underband circumference, bust circumference, biacromial breadth, acromiale-radiale length, sum of eight skinfolds.	0.021	X:0.58 Y:0.35 Z:0.09	0.34
10	BMI, waist-hip ratio, bust circumference, biacromial breadth, acromiale-radiale length, sum of eight skinfolds.	0.021	X:0.59 Y:0.35 Z:0.11	0.35

Note. <sup>†</sup>calculated as the Euclidean distance between the observed and model predicted position in the three-dimensional space.